Electroosmotic Flow Dipole: Experimental Observation and Flow Field Patterning

Federico Paratore,[1,2] Evgeniy Boyko,[2] Govind V. Kaigala,[1,*] and Moran Bercovici[2,3,†]
[1]IBM Research–Zurich, Säumerstrasse 4, 8803 Rüschlikon, Switzerland
[2]Faculty of Mechanical Engineering, Technion–Israel Institute of Technology, Haifa, 3200003 Israel
[3]Department of Mechanical Engineering, The University of Texas at Austin, Austin, Texas 78712, USA

(Received 21 December 2018; revised manuscript received 29 March 2019; published 7 June 2019)

We experimentally demonstrate the phenomenon of electroosmotic dipole flow that occurs around a localized surface charge region under the application of an external electric field in a Hele-Shaw cell. We use localized deposition of polyelectrolytes to create well-controlled surface charge variations, and show that, for a disk-shaped spot, the internal pressure distribution that arises results in uniform flow within the spot and dipole flow around it. We further demonstrate the superposition of surface charge spots to create complex flow patterns, without the use of physical walls.

DOI: 10.1103/PhysRevLett.122.224502

Electroosmotic flow (EOF) arises from the interaction of the ions in the electric double layer at a solid-liquid interface and an external electric field [1]. When the surface charge on the walls is inhomogeneous, nonuniform EOF arises. This phenomenon was extensively investigated in the field of capillary electrophoresis due to its undesired effect on sample dispersion [2–5]. The mechanism for dispersion was elucidated in the work of Herr *et al.* [6] which showed that as a result of the nonuniform EOF, an internal pressure gradient builds up in the capillary leading to a Poiseuille-type flow far from the surface charge discontinuity. Stroock *et al.* [7], using alternating stripes of different surface charges perpendicular to the electric field, showed that in the vicinity of the discontinuity mass conservation leads to flow recirculation.

The case of capillaries or microfluidic channels is a specific limit in which both the width and the depth of the fluidic configuration are significantly smaller than its length. A different limit is the case of nonuniform EOF in a microfluidic chamber where the two in-plane characteristic lengths are on the same order of magnitude. Boyko *et al.* [8] expanded on this concept and, based on previous theoretical formulations by Ajdari [9,10] and Long *et al.* [11], developed a theoretical framework to account for arbitrary zeta potential distributions on two parallel plates separated by thin-liquid film (Hele-Shaw cell). Their analysis predicted that a local nonuniformity in surface charge creates regions of higher and lower pressure, leading to in-plane recirculation, which for the case of a disk-shaped nonuniformity coincides precisely with dipole flow.

Here, we present an experimental study of nonuniform EOF in a Hele-Shaw configuration, confirming the existence of an electroosmotic flow dipole. We further show that, as expected from theory, superposition principles apply, and under combination of electric field and externally imposed uniform flow, the classical potential-flow solution of flow around a cylinder is retrieved [12,13]. This observation, in which streamlines can be curved without the use of physical walls, can potentially be leveraged as a mechanism for microscale flow patterning. In support of this, we demonstrate the ability to apply a desired surface charge distribution using polyelectrolytes, translating into the corresponding flow pattern.

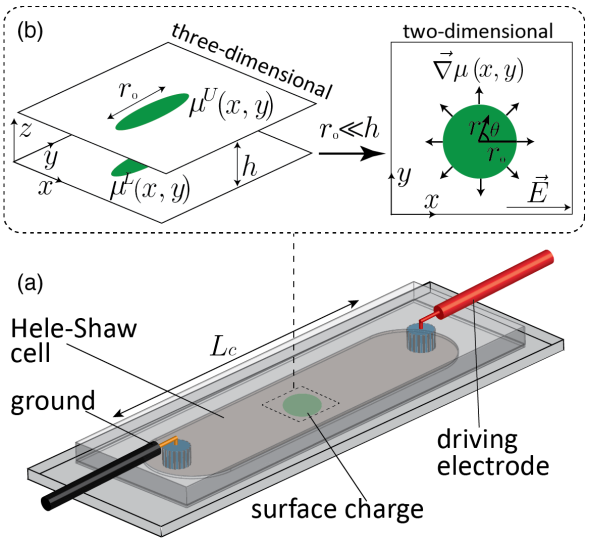

FIG. 1. Schematic of a Hele-Shaw cell with a patterned surface charge distribution. (a) The setup consists of two parallel plates, separated by a gap h. A finite region of characteristic length r_0 on the bottom plate is chemically altered to have a different electroosmotic wall mobility than its surrounding. An electrolyte is placed between the two plates and is subject to a uniform electric field E. The details of the chamber geometries are described in the Supplemental Material [14]. (b) Assuming lubrication conditions (i.e., for the case $h \ll r_0$), the system can be reduced to a two-dimensional system in which the equivalent electroosmotic distribution is the average between the upper and lower plate ones.

Figure 1 presents a schematic of our experimental setup designed to study the flow due to a localized surface charge nonuniformity in a Hele-Shaw chamber. The setup consists of two parallel plates (order of $L_c = 1$ cm) separated by a gap of $h = 15$ μm containing an aqueous solution; one of the plates is patterned with $r_0 =$ 100–500 μm diameter disk-shaped region having a modified zeta potential. In this way, the central assumption of a Hele-Shaw cell ($h \ll r_0 \ll L_c$), as used by Boyko *et al.* [8], holds. Furthermore, we use electrolytes with ionic strengths in the range of 1 to 50 mM, for which the assumption of a thin electric double layer regime [9,10] also holds and therefore the electrokinetic effects can be incorporated accounting for the slip velocity, which is described by the Helmholtz-Smoluchowski relation [1]

$$\vec{u}^i = \mu^i \vec{E} = -(\varepsilon \zeta^i/\eta)\vec{E}, \tag{1}$$

where μ^i is the electroosmotic (EO) wall mobility, ε is the dielectric permittivity of the liquid, η is its viscosity, $\vec{E}$ is electric field in the x-y plane and the superscript i indicates the upper (U) and lower (L) plates, respectively.

Under these conditions, the depth-averaged stream function $\psi = \psi(x, y)$ is governed by (see detailed derivation in the Supplemental Material [14]) [8]

$$\nabla_{\parallel}^2 \psi = (\vec{E} \times \vec{\nabla}_{\parallel} \bar{\mu}) \cdot \hat{z}, \tag{2}$$

where the subscript $\parallel$ indicates an operator in the x-y plane, $\hat{z}$ is the unitary vector in the z direction, and $\bar{\mu}$ is the arithmetic mean value of the EO wall mobilities, $\bar{\mu} = (\mu^L + \mu^U)/2$. We note that $-\nabla_{\parallel}^2 \psi$ also describes the depth-averaged vorticity.

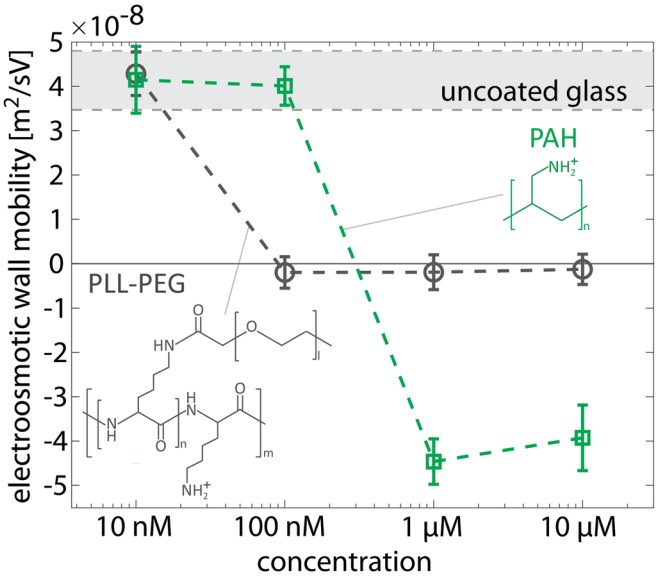

FIG. 2. Experimental measurements of EO wall mobility of a glass-PDMS microchannel uniformly coated with PAH or PLL-PEG as a function of their concentrations in the coating solution. Both PLL-PEG and PAH exhibit a sharp transition of the EO wall mobility for concentrations higher than a threshold. For the PAH case, a concentration between 100 nM and 1 μM is required to obtain an EO wall mobility of approximately -4.5×10^{-8} m^2/s V, thus fully inverting the native glass EO wall mobility. For the case of PLL-PEG, a concentration in the range 10 to 100 nM is sufficient to reduce the EO wall mobility to approximately -4.5×10^{-9} m^2/s V. The error bars and the gray area (uncoated channel) represent the 95% confidence interval of the mean of at least three different microchannels.

In a polar coordinate system, $(x, y) \to (r, \theta)$, where $r(x, y)$ is the radial vector with origin at the center of the disk and $\theta(x, y)$ is the angle between $r(x, y)$ and the x direction, we can solve Eq. (2) for the stream function,

$$\psi(r,\theta) = \begin{cases} -\left[\frac{1}{2}(\bar{\mu}_{\text{out}} - \bar{\mu}_{\text{in}})E\left(\frac{r_0}{r}\right)^2 - \bar{\mu}_{\text{out}}E + u_{\text{ext}}\right] r\sin\theta & r > r_0 \\ -\left[\frac{1}{2}(\bar{\mu}_{\text{out}} - \bar{\mu}_{\text{in}})E - \bar{\mu}_{\text{out}}E + u_{\text{ext}}\right] r\sin\theta & r \le r_0, \end{cases} \tag{3}$$

where $\bar{\mu}_{\text{in}}$ and $\bar{\mu}_{\text{out}}$ are the mean values of the EO wall mobilities inside and outside the disk, respectively. Here, u_{ext} is an additional (constant) degree of freedom that can be interpreted as a uniform velocity due to other forces such as an external pressure gradient. This equation represents a family of streamlines that can be expected to arise in the presence of a localized surface charge nonuniformity (see Supplemental Material Fig. S1).

Experimentally, one method to obtain such a surface charge distribution is by deposition of polyelectrolytes carrying a different charge than the native surface [7]. We use FITC-labeled poly(allylamine hydrochloride) (PAH), a cationic polyelectrolyte to impose a positive charge onto the negatively charged glass (the FITC label assists to visualize the patterns). Similarly, we use poly(L-lysine) grafted with poly(ethylene glycol) side chains (PLL-PEG) to screen the electric double layer in regions where we seek to eliminate the surface charge.

Figure 2 shows the characterization of the EO wall mobility as a function of the polyelectrolyte concentrations in the coating buffer (100 mM tris, 50 mM HCl, 100 mM NaCl (pH 8.2) [17] and 10 mM hepes, 5 mM NaOH

(pH 7.4) [18] for PAH and PLL-PEG, respectively). These experiments were performed using a 5 mM bistris, 2.5 mM HCl (pH 6.4) buffer containing neutral fluorescent 1 μm beads to trace the flow, with an applied electric field of 50 V/cm (see detailed procedure in Supplemental Material [14]). Both polyelectrolytes show a clear transition of the EO wall mobility for concentrations higher than a threshold. Deposition of PAH with concentrations higher than a value between 100 nM and 1 μM, translates into a EO wall mobility of approximately -4.5×10^{-8} m^2/s V, thus inverting the native glass EO wall mobility. Deposition of PLL-PEG with concentrations in the range 10 to 100 nM or higher reduces the EO wall mobility to approximately -4.5×10^{-9} m^2/s V, one order of magnitude smaller than the one produced by a PAH-coated glass.

Common methods to pattern surfaces with organic molecules (such as micromolding in capillaries [19,20] and its variants [21]) use a network of channels in conformal contact with the surface, through which the coating liquid is injected, replicating the channel network geometry as a surface pattern. These approaches are suitable only for patterns with connected topologies, e.g., for channels connected to a reservoir containing the coating agent. We seek to create more complex surface patterns, including ones with unconnected topology (e.g., isolated disks). Whereas such patterns could be achieved by microcontact printing [22] or photolithography, these require dedicated microfabricated molds. Instead, we use a microfluidic probe (MFP) [23], a noncontact scanning tool that confines hydrodynamically processing liquids in a micrometer-sized region between the probe and the target surface. This approach enables the formation of arbitrary surface patterns using the same tool. Figure 3 and Supplemental Movie S1 show the process of patterning using the MFP.

Figure 4 presents experimental and analytical streamlines generated by the disk-shaped PAH pattern, setting a positive EO wall mobility $\bar{\mu}_{\text{in}}$ within the disk, surrounded by PLL-PEG coating, setting an essentially zero wall EO mobility $\bar{\mu}_{\text{out}} \sim 0$ outside the disk (see Supplemental Movie S2). In the absence of an externally applied flow ($u_{\text{ext}} = 0$), we observe experimentally [Fig. 4(a)] the formation of an electroosmotic flow dipole outside the disk and uniform flow inside. This is in agreement with the analytical prediction [Eq. (3)] where the term $-\bar{\mu}_{\text{out}}E + u_{\text{ext}}$ is set to zero [Fig. 4(b)]. Our observation also confirms that the interaction between the electroosmotic flow dipole and an externally applied flow is predicted by superposition, as described by Eq. (3). Figure 4(c) shows the experimental flow field for the case of $u_{\text{ext}} = \bar{\mu}_{\text{in}}E/2$, in the direction opposing the flow within the disk; under this condition the depth-averaged velocity within the disk vanishes and, in agreement with theory [Fig. 4(d)], the streamlines curve around the spot, taking the shape of a flow around a cylinder.

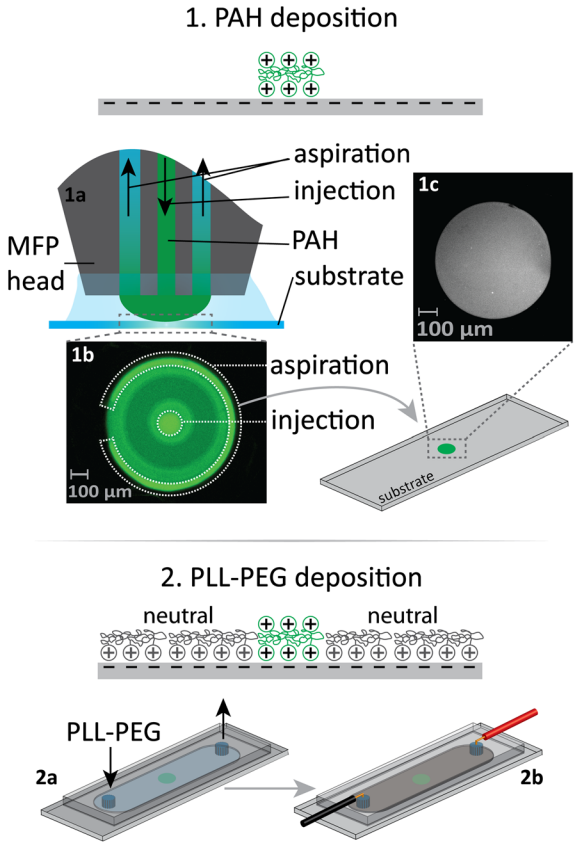

FIG. 3. Creation of zeta potential patterns using a microfluidic probe. (1) PAH, a positively charged polyelectrolyte, is deposited locally onto a negatively charged glass slide. (1a) Working principle of a microfluidic probe. The solution containing the polyelectrolytes is injected onto the surface through an injection channel while being aspirated out at a higher flow rate by one or more adjacent aspiration channels, creating a hydrodynamic flow confinement (HFC) at the apex of the MFP head. (1b) Raw fluorescence image of axisymmetric HFC using an injection channel surrounded by an aspiration ring while depositing FITC-labeled PAH. (1c) Fluorescence image of the resulting disk-shaped PAH-coated region. (2) The remaining surface is coated with PLL-PEG, a polyelectrolyte that results in an approximately zero surface charge. (2a) A microfluidic chamber is formed by a molded PDMS through which is flushed a solution containing the PLL-PEG. (2b) The chamber is filled with the working solution, and a uniform electric field is applied.

Superposition also holds well for other configurations. For example, Supplemental Material Fig. S2 shows the interaction of multiple dipoles which also can be well predicted by superposing multiple instances of solution [Eq. (3)] having different origins.

These observations suggest that beyond the fundamental study of microscale flow due to surface nonuniformities, deliberate nonuniform charge distribution can be used to engineer desired flow fields. Figure 5(a) illustrates the concepts of "writing" a surface charge distribution using polyelectrolyte deposition. Figure 5(b) presents the flow field resulting from a surface pattern displaying the text

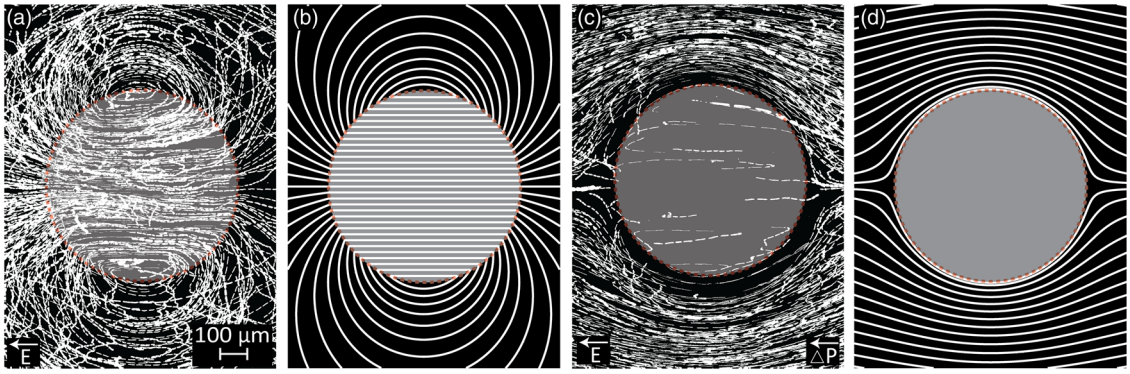

FIG. 4. Experimental and analytical flow streamlines generated by a disk with uniform zeta potential (PAH) surrounded by a neutral surface (PLL-PEG). (a),(b) With no imposed external pressure gradient, the flow is uniform in the inner region of the disk and takes the shape of a dipole in the outer region, with two vortices forming around each pole. Here, the electric field is ∼22 V/cm. (c),(d) The addition of a pressure gradient of approximately 0.1 mbar/cm stagnates the flow within the disk, and causes the streamlines to curve around it, despite the absence of any physical walls. This flow field coincides with the solution for potential flow around a cylinder. Experimental details are reported in the Supplemental Material [14].

"EOF!". Surface charge discontinuities parallel to the electric field result in pressure gradients and acceleration or deceleration of the flow—this can be observed, e.g., in streamlines expanding out as they move from PAH to PLL-PEG–coated regions. Surface charge discontinuities perpendicular to the electric field result in the creation of vorticity [as is evident from Eq. (2)], observable as localized circulations over the horizontal segments of the letters. Because the pattern can be deconstructed to a set of overlapping dipoles, all effects are local, and the total mass flux of this configuration remains zero. These complex patterns can be also well predicted by the theory as shown in Supplemental Material Fig. S3.

In this work, we investigated experimentally the nonuniform electroosmotic flow arising from surface charge nonuniformity in a Hele-Shaw cell configuration. A fundamental observation is that a spot of different surface charge gives rise to an internal pressure distribution which results in a planar electroosmotic flow dipole. We can expect that such elaborate flows would naturally occur in any surface containing charge nonuniformities under an electric field. The electroosmotic flow dipole is composed of an internal region of uniform velocity and an external region in which the velocity coincides with that of a pure dipole. Despite its difference from a pure dipole, we demonstrated that its superposition with an externally imposed flow yields the well-known solution of flow around a cylinder. Importantly this flow field, in which streamlines bend around a cylinder shape, is obtained in an entirely unobstructed chamber.

These observations suggest that it is possible to manipulate microscale flows in a Hele-Shaw chamber solely by imposing a surface charge distribution, without the use of physical walls or mechanical components.

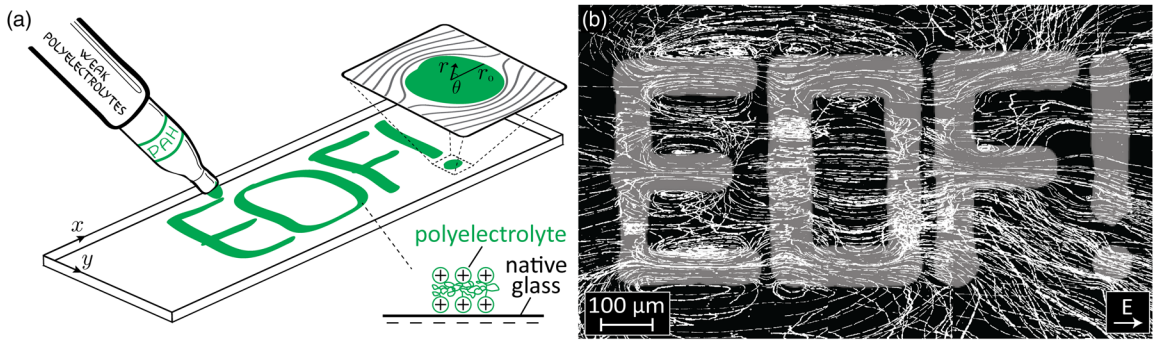

FIG. 5. Concept of creating complex flow fields by surface charge patterning. (a) Patterning of surface zeta potential by depositing weak polyelectrolytes using a microfluidic probe (represented by a marker pen in the sketch) displaying the text "EOF!". (b) Visualization of the resulting flow field. The EOF on the PAH patterned regions is directed from right to left. A variety of flow patterns can be obtained using such patterning, including flow divergence and convergence, counterrotating vortices, nested vortices, shear regions, stagnation points, and inflection points. The image is constructed by stitching of three images, each obtained by overlaying a fluorescence streakline image of the beads (TRITC filter) with a fluorescence images of the patterned surfaces (FITC filter). Here, the electric field is ∼30 V/cm.

We demonstrated this concept by using local deposition of polyelectrolytes and showed that a complex flow field can be realized. Two limitations of using polyelectrolyte deposition are that (i) only static flow configurations can be obtained and (ii) the number of zeta potential values are limited by the number of polyelectrolytes available. These limitations can likely be overcome by using gate electrodes [24] or optical means [25] to modify the surface charge dynamically, thus enabling a continuous range of surface charge values and dynamic control of the flow field. We believe that such advancements would allow the formation of tools and capabilities that simply cannot be created by conventional methods.

This project has received funding from the European Research Council (ERC) under the European Union's Horizon 2020 Research and Innovation Programme, grant agreement No. 678734 (MetamorphChip). This work was supported by the Initial Training Network, Virtual Vials, funded by the FP7 Marie Curie Actions of the European Commission (FP7-PEOPLE-2013-ITN-607322). E. B. is supported by the Adams Fellowship Program of the Israel Academy of Sciences and Humanities. We thank Prof. Abraham Stroock for useful discussions and advice on surface patterning. We thank X. van Kooten, D. Taylor, and R. Lovchik for useful discussions. F. P. and G. V. K. acknowledge E. Delamarche, W. Riess and H. E. Riel for continuous support.

*Corresponding author.
gov@zurich.ibm.com
†Corresponding author.
mberco@technion.ac.il

[1] R. J. Hunter, *Zeta Potential in Colloid Science: Principles and Applications* (Academic Press, London, 1988).
[2] P. Dutta and A. Beskok, Anal. Chem. **73**, 1979 (2001).
[3] S. Ghosal, J. Fluid Mech. **459**, 103 (2002).
[4] L.-M. Fu, J.-Y. Lin, and R.-J. Yang, J. Colloid Interface Sci. **258**, 266 (2003).
[5] L. Ren and D. Li, J. Colloid Interface Sci. **243**, 255 (2001).
[6] A. E. Herr, J. I. Molho, J. G. Santiago, M. G. Mungal, T. W. Kenny, and M. G. Garguilo, Anal. Chem. **72**, 1053 (2000).
[7] A. D. Stroock, M. Weck, D. T. Chiu, W. T. S. Huck, P. J. A. Kenis, R. F. Ismagilov, and G. M. Whitesides, Phys. Rev. Lett. **84**, 3314 (2000).
[8] E. Boyko, S. Rubin, A. D. Gat, and M. Bercovici, Phys. Fluids **27**, 102001 (2015).
[9] A. Ajdari, Phys. Rev. Lett. **75**, 755 (1995).
[10] A. Ajdari, Phys. Rev. E **53**, 4996 (1996).
[11] D. Long, H. A. Stone, and A. Ajdari, J. Colloid Interface Sci. **212**, 338 (1999).
[12] L. D. Landau and E. M. Lifshitz, *Fluid Mechanics* (Pergamon Press, Bristol, 1959).
[13] L. D. Landau and E. M. Lifshitz, *Electrodynamics of Continuous Media* (Pergamon Press, Bristol, 1960).
[14] See Supplemental Material at http://link.aps.org/supplemental/10.1103/PhysRevLett.122.224502 for detailed derivations of streamlines for disk-shaped and rectangular-shaped regions, experimental procedures, device geometries, supplemental figures and movies, and author contributions, which includes Refs. [15,16].
[15] L. G. Leal, *Advanced Transport Phenomena* (Cambridge University Press, Cambridge, England, 2007).
[16] G. L. Kenausis, J. Vörös, D. L. Elbert, N. Huang, R. Hofer, L. Ruiz-Taylor, M. Textor, J. A. Hubbell, and N. D. Spencer, J. Phys. Chem. B **104**, 3298 (2000).
[17] J. Choi and M. F. Rubner, Macromolecules **38**, 116 (2005).
[18] G. L. Kenausis, J. Vörös, D. L. Elbert, N. Huang, R. Hofer, L. Ruiz-Taylor, M. Textor, J. A. Hubbell, and N. D. Spencer, J. Phys. Chem. B **104**, 3298 (2000).
[19] E. Kim, Y. Xia, and G. M. Whitesides, Nature **376**, 581 (1995).
[20] E. Kim, Y. Xia, and G. M. Whitesides, J. Am. Chem. Soc. **118**, 5722 (1996).
[21] N. L. Jeon, I. S. Choi, B. Xu, and G. M. Whitesides, Adv. Mater. **11**, 946 (1999).
[22] S. A. Ruiz and C. S. Chen, Soft Matter **3**, 168 (2007).
[23] J. Autebert, J. F. Cors, D. P. Taylor, and G. V. Kaigala, Anal. Chem. **88**, 3235 (2016).
[24] R. B. M. Schasfoort, S. Schlautmann, J. Hendrikse, and A. van den Berg, Science **286**, 942 (1999).
[25] J. Moorthy, C. Khoury, J. S. Moore, and D. J. Beebe, Sens. Actuators B **75**, 223 (2001).